Polymer-stabilized blue phase liquid crystal display with slanted wall-shaped electrodes

Feng Zhou (周 凤), Qionghua Wang (王琼华)*, Di Wu (吴 迪), and Jianpeng Cui (崔建朋)

State Key Laboratory of Fundamental Science on Synthetic Vision, School of Electronics and Information Engineering, Sichuan University, Chengdu 610065, China

**Corresponding author: qhwang@scu.edu.cn*

Received June 7, 2011; accepted August 3, 2011; posted online September 22, 2011

A polymer-stabilized blue phase liquid crystal display (BPLCD) with slanted wall-shaped electrodes is proposed. Compared with the traditional BPLCD with wall-shaped electrodes, the electrodes of the proposed BPLCD are slightly angled to obtain phase retardation in the entire cell even at the position of electrodes. The proposed BPLCD demonstrates a relatively higher average transmittance and overall brightness than the traditional BPLCD.

OCIS codes: 230.3720, 160.3710.
doi: 10.3788/COL201210.022301.

Owing to the continuous improvement in image quality of liquid crystal displays (LCDs), they have been widely employed in desktop monitors, TVs, and mobile displays at present[1−5]. With the development of LCDs, the polymer-stabilized blue phase LCDs (BPLCDs)[6−11] can replace the conventional LCDs and become the next-generation display technology. The polymer-stabilized BPLCDs have numerous attractive features, such as submillisecond gray-to-gray response time, alignment-layer-free process, optically isotropic dark state, and cell gap insensitivity[12−14]. Because of these advantages, the fabrication processes of the BPLCDs are simplified, motion-image blurs are reduced, and color-sequential displays using RGB LEDs are enabled.

To reduce operating voltage and increase transmittance, various electrode configurations for BPLCDs have been proposed, such as protrusion electrode configuration, wall-shaped electrode configuration[12], corrugated electrode configuration[13], and so on. The wall-shaped electrode configuration produces uniformity in the induced birefringence between electrodes throughout the entire cell gap. BPLCDs with wall-shaped electrodes overcome the technical barriers of low transmittance and high operating voltage. However, no liquid crystal (LC) is placed above the wall-shaped electrodes to generate relative phase retardation. Hence, the transmittance above the electrodes is almost zero, which affects the brightness of the BPLCDs.

Thus, we propose a polymer-stabilized BPLCD with slanted wall-shaped electrodes. The electrodes of the proposed BPLCD have a slightly slanted angle relative to the traditional BPLCD with wall-shaped electrodes. Simulation results show that the proposed BPLCD has a higher aperture ratio and a relatively higher average transmittance than the traditional BPLCD.

Figure 1 shows the structure of the proposed BPLCD with slanted wall-shaped electrodes where P and C correspond to pixel and common electrodes, respectively. The dashed rectangles represent the traditional wall-shaped electrodes. The blue phase liquid crystal (BPLC) cell is sandwiched between two circular polarizers whose optical axes are orthogonal to each other. To obtain normally black mode, two broadband and wide-view circular polarizers consisting of positive and negative A-plates are employed[11,15]. The dimensions of the slanted wall-shaped electrodes are defined as follows: w is the electrode width, l is the spacing between two adjacent electrodes, d is the LC cell gap which is equal to the height of the traditional wall-shaped electrode, and θ is a small tilted angle relative to the traditional wall-shaped electrodes which corresponds to a horizontal shift s. All of the parameters are of the same size which simplifies the fabrication process.

For BPLCD, the induced birefringence is based on the Kerr effect[14,16]. At the voltage-off state, the cell shows a very good dark state because each small unit of the blue-phase cell is optically isotropic. At the voltage-on state, the cell exhibits a bright state because the induced birefringence takes place and the optic axis of the refractive ellipsoid aligns along the direction of the E vector. Thus, the BPLC becomes optically anisotropic. Such molecular reorientation results in a birefringence in the BPLC. The induced birefringence $(\Delta n)_{\text{ind}}$ can be expressed as[12,13]

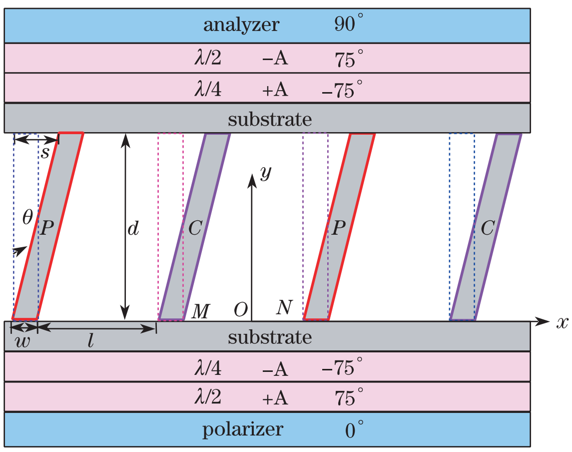

Fig. 1. Struture of the proposed BPLCD with slanted wall-shaped electrodes.

$$(\Delta n)_{\text{ind}} = \lambda K E^2 = (\Delta n)_0 (E/E_{\text{s}})^2, \quad (1)$$

where λ is the incident light wavelength, K is the Kerr constant, $(\Delta n)_0$ is the maximum induced birefringence, and E_{s} is the saturation field. The induced birefringence $(\Delta n)_{\text{ind}}$ is described as $(\Delta n)_{\text{ind}} = (\Delta n)_0 (E/E_{\text{s}})^2$ when $E < E_{\text{s}}$. It is also represented as $(\Delta n)_{\text{ind}} = (\Delta n)_0$ when $E \geqslant E_{\text{s}}$. There is an abrupt change to prevent divergence. In reality however, the induced birefringence gradually saturates as the electric field increases because all the LC directors are eventually reoriented by the electric field. To avoid this problem, the extended Kerr effect model is used. In this model, the induced birefringence $(\Delta n)_{\text{ind}}$ can be described as[16,17]

$$(\Delta n)_{\text{ind}} = (\Delta n)_{\text{sat}} \{1 - \exp[-(E/E_s)^2]\}, \quad (2)$$

where $(\Delta n)_{\text{sat}}$ is the saturated induced birefringence.

To evaluate the performance of the proposed structure, the electro-optic properties of the proposed BPLCD are simulated. The method is similar to the scheme described in Ref. [14]. First, COMSOL 3.5a software is used to obtain the distributions of the electric potential and the electric field E. Based on the electric field distribution, the distribution of the induced birefringence is calculated using Eq. (2) and the optic axis direction of each unit is assigned along the E vector. Subsequently, the electro-optic properties are calculated based on the extended Jones matrix methods[18]. In the simulations, the polymer-stabilized BPLC material has $K = 12.68$ nm/V^2, $(\Delta n)_{\text{sat}} = 0.2$, and $E_{\text{s}} = 5.6$ V/μm at $\lambda = 550$ nm[11]. The refractive index of the BPLC is 1.5 at isotropic state[19] and the dielectric anisotropy is assumed to remain constant under different voltages.

Figure 2 shows the simulated voltage-dependent transmittance (VT) curves of the traditional BPLCD at $\lambda = 550$ nm. In the simulation, four different electrode dimensions are compared. All the VT curves are normalized to the transmittance of the two polarizers (34.83%). In Fig. 2, as the electrode height achieves a larger value with unchanged electrode width and spacing, the operating voltage decreases and the transmittance increases. When the electrode spacing and height remain constant, the electrode width decreases and the transmittance increases while the operating voltage remains unchanged. However, the operating voltage and transmittance may decrease if the electrode width and height remain constant and the electrode spacing is reduced. Therefore, to achieve a low operating voltage and high optical efficiency, larger electrode spacing and larger height, but smaller electrode width should be maintained. For convenience, the electrode width $w = 2$ μm, electrode spacing $l = 5$ μm, and $d = 10$ μm are employed in the simulations.

Figure 3 shows the simulated VT curves with different horizontal shifts s at $\lambda = 550$ nm. In this case, s is varied from 0 to 6 μm. The peak of transmittance ranges from 67% to 80% (with corresponding operating voltage from 10 V_{RMS} to 12 V_{RMS}). Thus, the larger the horizontal shift s, the higher the average transmittance. However, a larger horizontal shift s can affect the fabrication of the LC cell; the process becomes more complicated and the operating voltage increases slightly. Based on the analysis, this is caused by the uneven distribution of the electric field at the edges of the electrodes. The oblique of the electrodes enlarges the non-uniform area. Moreover, the area of the non-uniform electric field gradually increases with the increase of the horizontal shift s. On the other hand, the horizontal electric field is reduced when the voltage of the BPLC cell remains constant. From the two points, the utilization of the electric field is decreased. Thus, the applied voltage increases with the increase in the horizontal shift s. This facilitates obtaining the same phase retardation as the horizontal shift $s = 0$ μm. Generally, the slanted wall-shaped electrodes tilted at a small angle can help to increase the transmittance and the overall brightness of BPLCDs.

Figure 4 shows the transmittance with respect to the position in a single electrode period for a BPLC cell. The curves with different values of horizontal shift s are simulated at the corresponding peak voltage V_{p} of the maximum transmittance, as shown in Fig. 3 ($s = 0$ μm V_{p} ~10 V_{RMS}, $s = 2$ μm V_{p} ~10.8 V_{RMS}, $s = 4$ μm V_{p} ~11.7 V_{RMS}, $s = 6$ μm V_{p} ~12 V_{RMS}). As shown in Fig. 1, M and N are the right corner and the left corner of the adjacent wall-shaped electrodes, respectively. O is the midpoint of M and N and the coordinate origin. The x-axis and the y-axis are defined as parallel to the substrate and vertical to the substrate, respectively. Figure 4 shows that the transmittance at the location of the traditional wall-shaped electrodes ($s = 0$ μm) is zero, which affects the overall brightness of the entire BPLC cell. Because the electrode configuration of the proposed BPLCD has a slightly slanted angle, the BPLCs are filled in the BPLC cell, even at the location of the

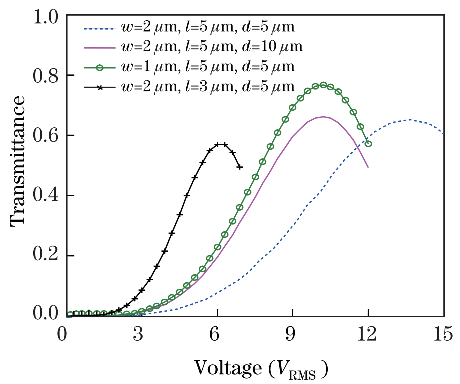

Fig. 2. Simulation VT curves with different wall-shaped electrode configurations.

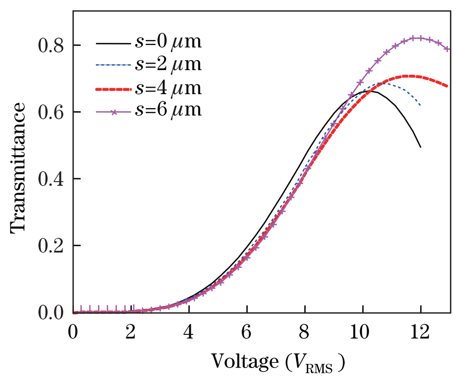

Fig. 3. Simulation VT curves with different horizontal shifts s of the slanted wall-shaped electrodes.

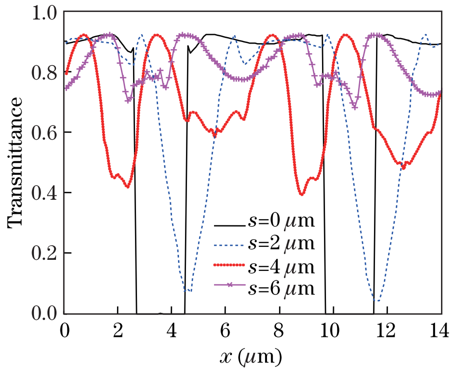

Fig. 4. Simulation transmittance curves with respect to the position in a single electrode period for a BPLC cell with different horizontal shifts s.

slanted wall-shaped electrodes. The proposed BPLCD obtains phase retardation anywhere in the BPLC cell. Therefore, the transmittance of the proposed BPLCD with slanted wall-shaped electrodes occurs everywhere in the BPLC cell, although the transmittance at the location of the electrodes is lower than that at the other place. As shown in Fig. 4, the area of the maximum transmittance decreases when the horizontal shift s increases. This is caused by the increase of the area of the electrodes along the direction of the x-axis. An added reason is the transmittance at the location of the electrodes which is lower compared with the other area due to the oblique of the electrodes. However, as the horizontal shift s increases from 0 to 6 μm, the transmittance at the location of electrodes increases from 0% to 68%, which results in the improvement of the average transmittance, as shown in Fig. 3. Therefore, if the aperture is defined as the place where the transmittance exceeds 25% of the maximum intensity[20], we can state that the proposed BPLCD with slanted wall-shaped electrode configuration effectively improves the aperture ratio.

In conclusion, we propose a polymer-stabilized BPLCD with slanted wall-shaped electrodes. In this device, wall-shaped electrodes are tilted with a small angle. The slanted wall-shaped electrode configuration enables the transmittance to occur everywhere in the BPLCD, which facilitates improvement of the brightness of the traditional BPLCDs with wall-shaped electrode configuration. The fabrication process is simplified because the same electrode dimension, gap, and tilted angle are employed. Although the slightly tilted electrodes complicate the fabrication process to a certain degree, the device exhibits a relatively high transmittance which occurs everywhere and increases the overall brightness.

This work was supported by the National Natural Science Foundation of China under Nos. 60877004 and 61036008.

References

1. H. Y. Kim, Z. Ge, S. T. Wu, and S. H. Lee, App. Phys. Lett. **91,** 231108 (2007).
2. S. H. Lee, H. W. Do, G. D. Lee, T. H. Yoon, and J. C. Kim, Jpn. J. Appl. Phys. **42,** L1455 (2003).
3. X. Zhu, Z. Ge, T. X. Wu, and S. T. Wu, J. Disp. Technol. **1,** 15 (2005).
4. Z. Ge, X. Zhu, T. X. Wu, S. T. Wu, W. Y. Li, and C. K. Wei, J. Soc. Inf. Disp. **17,** 561 (2009).
5. Y. Li, Z. Ge, and S. T. Wu, J. Disp. Technol. **5,** 319 (2009).
6. H. Kikuchi, M. Yokota, Y. Hiskado, H. Yang, and T. Kajiyama, Nat. Mater. **1,** 64 (2002).
7. Y. Haseba, H. Kikuchi, T. Nagamura, and T. Kajiyama, Adv. Mater. **17,** 2311 (2005).
8. Y. Hisakado, H. Kikuchi, T. Nagamura, and T. Kajiyama, Adv. Mater. **17,** 96 (2005).
9. S. W. Choi, S. I. Yamamoto, Y. Haseba, H. Higuchi, and H. Kikuchi, Appl. Phys. Lett. **92,** 043119 (2008).
10. Z. Ge, S. Gauza, M. Jiao, H. Xianyu, and S. T. Wu, Appl. Phys. Lett. **94,** 101104 (2009).
11. Y. Li, M. Jiao, and S. T. Wu, Opt. Express **18,** 16486 (2010).
12. M. Kim, M. S. Kim, B. G. Kang, M. K. Kim, S. Yoon, S. H. Lee, Z. Ge, L. Rao, S. Gauza, and S. T. Wu, J. Phys. D: Appl. Phys. **42,** 235502 (2009).
13. M. Jiao, Y. Li, and S. T. Wu, Appl. Phys. Lett. **96,** 011102 (2010).
14. Z. Ge, L. Rao, S. Gauza, and S. T. Wu, J. Disp. Technol. **5,** 250 (2009).
15. Z. Ge, M. Jiao, R. Lu, T. X. Wu, S. T. Wu, W. Y. Li, and C. K. Wei, J. Disp. Technol. **4,** 129 (2008).
16. J. Yan, H. C. Cheng, S. Gauza, Y. Li, M. Jiao, L. Rao, and S. T. Wu, Appl. Phys. Lett. **96,** 071105 (2010).
17. H. C. Cheng, J. Yan, T. Ishinabe, and S. T. Wu, Appl. Phys. Lett. **98,** 261102 (2011).
18. Z. Ge, T. X. Wu, X. Zhu, and S. T. Wu, J. Opt. Soc. Am. A **22,** 966 (2005).
19. J. Yan, M. Jiao, L. Rao, and S. T. Wu, Opt. Express **18,** 11450 (2010).
20. S. Yoon, M. Kim, M. S. Kim, B. G. Kang, M. K. Kim, A. K. Srivastava, S. H. Lee, Z. Ge, L. Rao, S. Gauza, and S. T. Wu, Liq. Cryst. **37,** 201 (2010).